Observation of Exclusive Two-Body B Decays to Kaons and Pions

R. Godang,[1] K. Kinoshita,[1] I. C. Lai,[1] P. Pomianowski,[1] S. Schrenk,[1] G. Bonvicini,[2] D. Cinabro,[2] R. Greene,[2] L. P. Perera,[2] G. J. Zhou,[2] M. Chadha,[3] S. Chan,[3] G. Eigen,[3] J. S. Miller,[3] C. O'Grady,[3] M. Schmidtler,[3] J. Urheim,[3] A. J. Weinstein,[3] F. Würthwein,[3] D. W. Bliss,[4] G. Masek,[4] H. P. Paar,[4] S. Prell,[4] V. Sharma,[4] D. M. Asner,[5] J. Gronberg,[5] T. S. Hill,[5] D. J. Lange,[5] R. J. Morrison,[5] H. N. Nelson,[5] T. K. Nelson,[5] D. Roberts,[5] A. Ryd,[5] R. Balest,[6] B. H. Behrens,[6] W. T. Ford,[6] A. Gritsan,[6] H. Park,[6] J. Roy,[6] J. G. Smith,[6] J. P. Alexander,[7] R. Baker,[7] C. Bebek,[7] B. E. Berger,[7] K. Berkelman,[7] K. Bloom,[7] V. Boisvert,[7] D. G. Cassel,[7] D. S. Crowcroft,[7] M. Dickson,[7] S. von Dombrowski,[7] P. S. Drell,[7] K. M. Ecklund,[7] R. Ehrlich,[7] A. D. Foland,[7] P. Gaidarev,[7] R. S. Galik,[7] L. Gibbons,[7] B. Gittelman,[7] S. W. Gray,[7] D. L. Hartill,[7] B. K. Heltsley,[7] P. I. Hopman,[7] J. Kandaswamy,[7] P. C. Kim,[7] D. L. Kreinick,[7] T. Lee,[7] Y. Liu,[7] N. B. Mistry,[7] C. R. Ng,[7] E. Nordberg,[7] M. Ogg,[7,*] J. R. Patterson,[7] D. Peterson,[7] D. Riley,[7] A. Soffer,[7] B. Valant-Spaight,[7] C. Ward,[7] M. Athanas,[8] P. Avery,[8] C. D. Jones,[8] M. Lohner,[8] S. Patton,[8] C. Prescott,[8] J. Yelton,[8] J. Zheng,[8] G. Brandenburg,[9] R. A. Briere,[9] A. Ershov,[9] Y. S. Gao,[9] D. Y.-J. Kim,[9] R. Wilson,[9] H. Yamamoto,[9] T. E. Browder,[10] Y. Li,[10] J. L. Rodriguez,[10] T. Bergfeld,[11] B. I. Eisenstein,[11] J. Ernst,[11] G. E. Gladding,[11] G. D. Gollin,[11] R. M. Hans,[11] E. Johnson,[11] I. Karliner,[11] M. A. Marsh,[11] M. Palmer,[11] M. Selen,[11] J. J. Thaler,[11] K. W. Edwards,[12] A. Bellerive,[13] R. Janicek,[13] D. B. MacFarlane,[13] P. M. Patel,[13] A. J. Sadoff,[14] R. Ammar,[15] P. Baringer,[15] A. Bean,[15] D. Besson,[15] D. Coppage,[15] C. Darling,[15] R. Davis,[15] S. Kotov,[15] I. Kravchenko,[15] N. Kwak,[15] L. Zhou,[15] S. Anderson,[16] Y. Kubota,[16] S. J. Lee,[16] J. J. O'Neill,[16] R. Poling,[16] T. Riehle,[16] A. Smith,[16] M. S. Alam,[17] S. B. Athar,[17] Z. Ling,[17] A. H. Mahmood,[17] S. Timm,[17] F. Wappler,[17] A. Anastassov,[18] J. E. Duboscq,[18] D. Fujino,[18,†] K. K. Gan,[18] T. Hart,[18] K. Honscheid,[18] H. Kagan,[18] R. Kass,[18] J. Lee,[18] M. B. Spencer,[18] M. Sung,[18] A. Undrus,[18,‡] R. Wanke,[18] A. Wolf,[18] M. M. Zoeller,[18] B. Nemati,[19] S. J. Richichi,[19] W. R. Ross,[19] H. Severini,[19] P. Skubic,[19] M. Bishai,[20] J. Fast,[20] J. W. Hinson,[20] N. Menon,[20] D. H. Miller,[20] E. I. Shibata,[20] I. P. J. Shipsey,[20] M. Yurko,[20] S. Glenn,[21] S. D. Johnson,[21] Y. Kwon,[21,§] S. Roberts,[21] E. H. Thorndike,[21] C. P. Jessop,[22] K. Lingel,[22] H. Marsiske,[22] M. L. Perl,[22] V. Savinov,[22] D. Ugolini,[22] R. Wang,[22] X. Zhou,[22] T. E. Coan,[23] V. Fadeyev,[23] I. Korolkov,[23] Y. Maravin,[23] I. Narsky,[23] V. Shelkov,[23] J. Staeck,[23] R. Stroynowski,[23] I. Volobouev,[23] J. Ye,[23] M. Artuso,[24] F. Azfar,[24] A. Efimov,[24] M. Goldberg,[24] D. He,[24] S. Kopp,[24] G. C. Moneti,[24] R. Mountain,[24] S. Schuh,[24] T. Skwarnicki,[24] S. Stone,[24] G. Viehhauser,[24] X. Xing,[24] J. Bartelt,[25] S. E. Csorna,[25] V. Jain,[25,‖] K. W. McLean,[25] and S. Marka[25]

(CLEO Collaboration)

[1]*Virginia Polytechnic Institute and State University, Blacksburg, Virginia 24061*
[2]*Wayne State University, Detroit, Michigan 48202*
[3]*California Institute of Technology, Pasadena, California 91125*
[4]*University of California, San Diego, La Jolla, California 92093*
[5]*University of California, Santa Barbara, California 93106*
[6]*University of Colorado, Boulder, Colorado 80309-0390*
[7]*Cornell University, Ithaca, New York 14853*
[8]*University of Florida, Gainesville, Florida 32611*
[9]*Harvard University, Cambridge, Massachusetts 02138*
[10]*University of Hawaii at Manoa, Honolulu, Hawaii 96822*
[11]*University of Illinois, Urbana-Champaign, Illinois 61801*
[12]*Carleton University, Ottawa, Ontario, Canada K1S 5B6, and the Institute of Particle Physics, Montréal, Québec, Canada*
[13]*McGill University, Montréal, Québec, Canada H3A 2T8, and the Institute of Particle Physics, Montréal, Québec, Canada*
[14]*Ithaca College, Ithaca, New York 14850*
[15]*University of Kansas, Lawrence, Kansas 66045*
[16]*University of Minnesota, Minneapolis, Minnesota 55455*
[17]*State University of New York at Albany, Albany, New York 12222*
[18]*The Ohio State University, Columbus, Ohio 43210*
[19]*University of Oklahoma, Norman, Oklahoma 73019*
[20]*Purdue University, West Lafayette, Indiana 47907*
[21]*University of Rochester, Rochester, New York 14627*
[22]*Stanford Linear Accelerator Center, Stanford University, Stanford, California 94309*
[23]*Southern Methodist University, Dallas, Texas 75275*
[24]*Syracuse University, Syracuse, New York 13244*
[25]*Vanderbilt University, Nashville, Tennessee 37235*

(Received 17 November 1997)

We have studied two-body charmless hadronic decays of B mesons into the final states $\pi\pi$, $K\pi$, and KK. Using 3.3×10^6 $B\overline{B}$ pairs collected with the CLEO-II detector, we have made the first observation

 0031-9007/98/80(16)/3456(5)$15.00

of the decay $B^0 \to K^+\pi^-$, the sum of $B^+ \to \pi^+\pi^0$ and $B^+ \to K^+\pi^0$ decays, and see strong evidence for the decay $B^+ \to K^0\pi^+$ (an average over charge-conjugate states is always implied). We place upper limits on branching fractions for the remaining decay modes. [S0031-9007(98)05799-8]

PACS numbers: 13.25.Hw, 11.30.Er, 14.40.Nd

The phenomenon of *CP* violation, so far observed only in the neutral kaon system, can be accommodated by a complex phase in the Cabibbo-Kobayashi-Maskawa quark-mixing matrix [1]. Whether this phase is the correct, or only, source of *CP* violation awaits experimental confirmation. *B* meson decays, in particular, charmless *B* meson decays, will play an important role in verifying this picture.

The decay $B^0 \to \pi^+\pi^-$, dominated by the $b \to u$ tree diagram [Fig. 1(a)], can be used to measure *CP* violation due to B^0-$\overline{B}^0$ mixing at both asymmetric *B* factories and hadron colliders. However, theoretical uncertainties due to the presence of the $b \to dg$ penguin diagram [Fig. 1(b)] make it difficult to extract the angle α of the unitarity triangle from $B^0 \to \pi^+\pi^-$ alone. Additional measurements of $B^+ \to \pi^+\pi^0$, $B^0 \to \pi^0\pi^0$, and the use of isospin symmetry may resolve these uncertainties [2].

$B \to K\pi$ decays are dominated by the $b \to sg$ gluonic penguin diagram, with additional contributions from $b \to u$ tree and color-allowed electroweak penguin [Fig. 1(d)] processes. Interference between the penguin and spectator amplitudes can lead to direct *CP* violation, which would manifest itself as a rate asymmetry for decays of *B* and $\overline{B}$ mesons. Recently, the ratio $R = \mathcal{B}(B \to K^\pm\pi^\mp)/\mathcal{B}(B^\pm \to K^0\pi^\pm)$ was shown [3] to constrain γ, the phase of V_{ub}. Several methods of measuring γ using only decay rates of $B \to K\pi$, $\pi\pi$ processes were also proposed [4]. This is particularly important, as γ is the least known parameter of the unitarity triangle and is likely to remain the most difficult to determine experimentally. This Letter describes the first measurement of exclusive charmless hadronic *B* decays. Previous measurements existed only for the sum of several two-body final states [5,6].

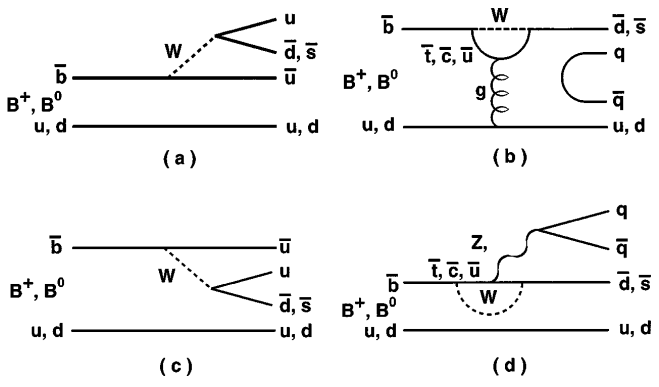

FIG. 1. The dominant decay processes are expected to be (a) external *W*-emission, (b) gluonic penguin, (c) internal *W*-emission, and (d) external electroweak penguin.

The data set used in this analysis was collected with the CLEO-II detector at the Cornell Electron Storage Ring (CESR). It consists of 3.14 fb^{-1} taken at the $\Upsilon(4S)$ (on-resonance) and 1.62 fb^{-1} taken below $B\overline{B}$ threshold. The on-resonance sample contains 3.3×10^6 $B\overline{B}$ pairs. The below-threshold sample is used for continuum background studies.

CLEO-II is a general purpose solenoidal magnet detector, described in detail elsewhere [7]. The momenta of charged particles are measured in a tracking system consisting of a 6-layer straw tube chamber, a 10-layer precision drift chamber, and a 51-layer main drift chamber, all operating inside a 1.5 T superconducting solenoid. The main drift chamber also provides a measurement of the specific ionization loss, dE/dx, used for particle identification. Photons are detected using a 7800-crystal CsI(Tl) electromagnetic calorimeter. Muons are identified using proportional counters placed at various depths in the steel return yoke of the magnet.

Charged tracks are required to pass track quality cuts based on the average hit residual and the impact parameters in both the r-ϕ and r-z planes. Pairs of tracks with vertices displaced by at least 3 mm from the primary interaction point are taken as K_S^0 candidates. We require the $\pi^+\pi^-$ invariant mass to be within 10 MeV, 2 standard deviations (σ), of the K_S^0 mass. Isolated showers with energies greater than 30 MeV in the central region of the CsI calorimeter and greater than 50 MeV elsewhere, are defined to be photons. Pairs of photons with an invariant mass within 20 MeV ($\sim 2\sigma$) of the nominal π^0 mass are kinematically fitted with the mass constrained to the π^0 mass. To reduce combinatoric backgrounds we require the lateral shapes of the showers to be consistent with those from photons, and that $|\cos\theta^*| < 0.97$, where θ^* is the angle between the direction of flight of the π^0 and the photons in the π^0 rest frame.

Charged particles are identified as kaons or pions using dE/dx. Electrons are rejected based on dE/dx and the ratio of the track momentum to the associated shower energy in the CsI calorimeter. We reject muons by requiring that the tracks do not penetrate the steel absorber to a depth greater than five nuclear interaction lengths. We have studied the dE/dx separation between kaons and pions for momenta $p \sim 2.6$ GeV/c in data using D^{*+}-tagged $D^0 \to K^-\pi^+$ decays; we find a separation of $(1.7 \pm 0.1)\sigma$.

We calculate a beam-constrained *B* mass $M = \sqrt{E_b^2 - p_B^2}$, where p_B is the *B* candidate momentum and E_b is the beam energy. The resolution in *M* ranges from 2.5 to 3.0 MeV/c^2, where the larger resolution corresponds to decay modes with π^0's. We define $\Delta E = E_1 + E_2 - E_b$, where E_1 and E_2 are the

TABLE I. Experimental results and theoretical predictions [11]. Branching fractions ($\mathcal{B}$) and 90% C.L. upper limits are given in 10^{-5} units. Quoted significance of the fit results is statistical only. The errors on $\mathcal{B}$ are statistical, fit systematics, and efficiency systematics, respectively. We quote upper limits with (and without) the systematics taken into account.

Mode	N_S	Sig.	$\mathcal{E}(\%)$	$\mathcal{B}$	Theory $\mathcal{B}$
$\pi^+\pi^-$	$9.9^{+6.0}_{-5.1}$	2.2σ	44 ± 3	<1.5(1.3)	0.8–2.6
$\pi^+\pi^0$	$11.3^{+6.3}_{-5.2}$	2.8σ	37 ± 3	<2.0(1.6)	0.4–2.0
$\pi^0\pi^0$	$2.7^{+2.7}_{-1.7}$	2.4σ	29 ± 3	<0.93(0.74)	0.006–0.1
$K^+\pi^-$	$21.6^{+6.8}_{-6.0}$	5.6σ	44 ± 3	$1.5^{+0.5}_{-0.4} \pm 0.1 \pm 0.1$	0.7–2.4
$K^+\pi^0$	$8.7^{+5.3}_{-4.2}$	2.7σ	37 ± 3	<1.6(1.3)	0.3–1.3
$K^0\pi^+$	$9.2^{+4.3}_{-3.8}$	3.2σ	12 ± 1	$2.3^{+1.1}_{-1.0} \pm 0.3 \pm 0.2$	0.8–1.5
$K^0\pi^0$	$4.1^{+3.1}_{-2.4}$	2.2σ	8 ± 1	<4.1(3.3)	0.3–0.8
K^+K^-	$0.0^{+1.3}_{-0.0}$	0.0σ	44 ± 3	<0.43(0.35)	···
$K^+\overline{K}^0$	$0.6^{+3.8}_{-0.6}$	0.2σ	12 ± 1	<2.1(1.7)	0.07–0.13
$K^0\overline{K}^0$	0	···	5 ± 1	<1.7(1.5)	0.07–0.12
$h^+\pi^0$	$20.0^{+6.8}_{-5.9}$	5.5σ	37 ± 3	$1.6^{+0.6}_{-0.5} \pm 0.3 \pm 0.2$	···

energies of the daughters of the B meson candidate. The resolution on ΔE is mode dependent and ranges from ± 26 MeV for $K^0_S\pi^+$ to $+82/-162$ MeV for $\pi^0\pi^0$. The latter resolution is asymmetric because of energy loss out of the back of the CsI crystals. The energy constraint also helps to distinguish between modes of the same topology. For example, ΔE for $B^0 \to K^+\pi^-$, calculated assuming $B^0 \to \pi^+\pi^-$, has a distribution that is centered at -42 MeV, giving a separation of 1.6σ between $B^0 \to K^+\pi^-$ and $B^0 \to \pi^+\pi^-$. We accept events with M within 5.2–5.3 GeV/c^2 and $|\Delta E| < 200$ (300) MeV for decay modes without (with) a π^0 in the final state. This fiducial region includes the signal region, and a sideband for background determination.

We have studied backgrounds from $b \to c$ decays and other $b \to u$ and $b \to s$ decays and find that all are negligible for the analyses presented here. The main background arises from $e^+e^- \to q\overline{q}$ (where $q = u, d, s, c$). Such events typically exhibit a two-jet structure and can produce high momentum back-to-back tracks in the fiducial region. To reduce contamination from these events, we calculate the angle θ_S between the sphericity axis of the candidate tracks and showers [8] and the sphericity axis of the rest of the event. The distribution of $\cos\theta_S$ is strongly peaked at ± 1 for $q\overline{q}$ events and is nearly flat for $B\overline{B}$ events. We require $|\cos\theta_S| < 0.8$ which eliminates 83% of the background. Using a detailed GEANT-based Monte Carlo simulation [9] we determine overall detection efficiencies ($\mathcal{E}$) of 5%–44%, as listed in Table I. Efficiencies contain branching fractions for $K^0 \to K^0_S \to \pi^+\pi^-$ and $\pi^0 \to \gamma\gamma$ where applicable. We estimate a systematic error on the efficiency using independent data samples.

Additional discrimination between signal and $q\overline{q}$ background is provided by a Fisher discriminant technique as described in detail in Ref. [5]. The Fisher discriminant is a linear combination $\mathcal{F} \equiv \sum_{i=1}^{N} \alpha_i y_i$, where the coefficients α_i are chosen to maximize the separation between the signal and background Monte Carlo samples. The 11 inputs, y_i, are $|\cos\theta_{\rm cand}|$ (the cosine of the angle between the candidate sphericity axis and beam axis), the ratio of Fox-Wolfram moments H_2/H_0 [10], and nine variables that measure the scalar sum of the momenta of tracks and showers from the rest of the event in nine angular bins, each of 10°, centered about the candidate's sphericity axis.

For all modes except $B^0 \to K^0\overline{K}^0$ we perform unbinned maximum-likelihood (ML) fits using ΔE, M, $\mathcal{F}$, $|\cos\theta_B|$ (the angle between the B meson momentum and beam axis), and dE/dx (where applicable) as input information for each candidate event to determine the signal yields. Five different fits are performed, one for each topology (h^+h^-, $h^+\pi^0$, $\pi^0\pi^0$, $h^+K^0_S$, and $K^0_S\pi^0$, $h^\pm$ referring to a charged kaon or pion). In each of these fits the likelihood of the event is parametrized by the sum of probabilities for all relevant signal and background hypotheses, with relative weights determined by maximizing likelihood function ($\mathcal{L}$). The probability of a particular hypothesis is calculated as a product of the probability density functions (PDF's) for each of the input variables. The PDF's of the input variables are parametrized by a Gaussian, a bifurcated Gaussian, or a sum of two bifurcated Gaussians, except for $|\cos\theta_B|$ ($1 - |\cos\theta_B|^2$ for signal, constant for background), background ΔE (straight line), and background M [$f(M) \propto M\sqrt{1-x^2}\,\exp[-\gamma(1-x^2)]$; $x = M/E_b$] [12].

The parameters for the PDF's are determined from independent data and high-statistics Monte Carlo samples. We estimate a systematic error on the fitted yield by varying the PDF's used in the fit. The error is dominated by the limited statistics in the independent data samples we used to determine the PDF's. Further details about the likelihood fit can be found in Ref. [5]. In order to see how systematic uncertainties affect statistical significance of our signals, we repeated the fit for the h^+h^-, $h^+\pi^0$,

and $h^+K_S^0$ modes with all fit parameters changed by their systematic error to maximally reduce the overall signal yield. Under these conditions, the significance of the $K^+\pi^-$, $h^+\pi^0$, and $K_S^0\pi^+$ signals becomes 4.9, 4.6, and 2.9 σ respectively.

Figure 2 shows contour plots of $-2\ln\mathcal{L}$ for the ML fits to the signal yields (N). The curves represent the $n\sigma$ contours ($n = 1$–5), which correspond to the increase in $-2\ln\mathcal{L}$ by n^2. The dashed curve marks the 3σ contour. The statistical significance of a given signal yield is determined by repeating the fit with the signal yield fixed to be zero and recording the change in $-2\ln\mathcal{L}$. To further illustrate the fits, Fig. 3 shows M (ΔE) projections for events in a signal region defined by $|\Delta E| < 2\sigma_{\Delta E}$($|M - 5.28| < 2\sigma_M$). We also make a cut on $\mathcal{F}$ which keeps 67% of the signal and rejects 80% of the background. For Fig. 3(a), events are sorted by dE/dx according to the most likely hypothesis. For Fig. 3(c), 3σ consistency with the pion hypothesis is required. Overlaid on these plots are the projections of the PDF's used in the fit, normalized according to the fit results multiplied by the efficiency of the additional cuts (~60%–70% for the signal and ~2%–10% for the background). The central values of the signal yields from the fits (N_S) are given in Table I. We find statistically significant signals for the decay $B^0 \to K^+\pi^-$ and the sum of decays $B^+ \to K^+\pi^0$ and $B^+ \to \pi^+\pi^0$, and see strong evidence for the decay $B^+ \to K^0\pi^+$.

As a cross-check, we perform a counting analysis in the modes $B^0 \to K^+\pi^-$, $B^+ \to K^0\pi^+$, and $B^+ \to h^+\pi^0$. We calculate the probability of the background fluctuation to produce the excess of events shown in Fig. 3 to be 2.0×10^{-7} for the $K^+\pi^-$ mode, 1.6×10^{-3} for the $h^+\pi^0$ mode, and 2.5×10^{-4} for the $K^0\pi^+$ mode.

The statistical significance of the fitted yields in the modes $\pi^+\pi^-$, $\pi^+\pi^0$, $\pi^0\pi^0$, $K^+\pi^0$, and $K^0\pi^0$ ranges from 2.2σ to 2.8σ. We consider these to be not statistically significant and calculate 90% confidence level (C. L.) upper limit yields by integrating the likelihood function

$$\frac{\int_0^{N^{UL}} \mathcal{L}_{\max}(N)\,dN}{\int_0^{\infty} \mathcal{L}_{\max}(N)\,dN} = 0.90\,, \qquad (1)$$

where $\mathcal{L}_{\max}(N)$ is the maximum $\mathcal{L}$ at fixed N to conservatively account for possible correlations among the free parameters in the fit. We then increase upper limit yields by their systematic errors and reduce detection efficiencies by their systematic errors to calculate branching fraction upper limits given in Table I.

We search for the decay $B^0 \to K^0\overline{K}^0$ via $K^0, \overline{K}^0 \to K_S^0 \to \pi^+\pi^-$. Since the background for this decay is quite low, the complication of a ML fit is not necessary and a simple counting analysis is used. Event selection is as described above, except no Fisher discriminant is used and $|\cos\theta_T| < 0.75$ cut is applied ($\cos\theta_T$ is defined similar to $\cos\theta_S$, but with thrust axis [8] used instead of sphericity). We define the signal region by requiring $|\Delta E| < 65$ MeV (2.5σ), and $|M - 5.28| < 0.005$ GeV/c^2 (2.4σ). We observe no events in the signal region and calculate a 90% C. L. branching fraction upper limit of $\mathcal{B}(B^0 \to K^0\overline{K}^0) < 1.7 \times 10^{-5}$.

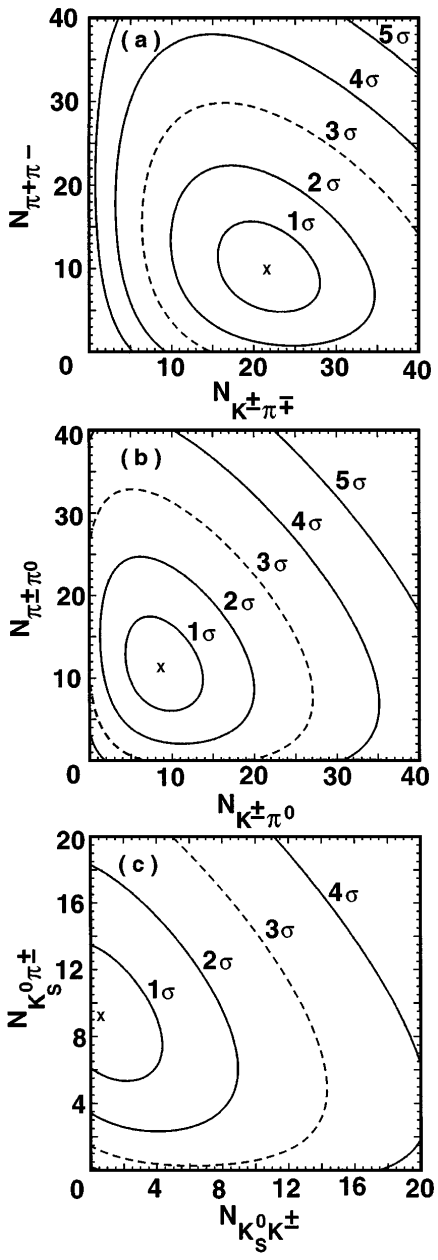

FIG. 2. Contours of the $-2\ln\mathcal{L}$ for the ML fits to (a) $N_{K^\pm\pi^\mp}$ and $N_{\pi^+\pi^-}$ for $B^0 \to K^+\pi^-$ and $B^0 \to \pi^+\pi^-$, (b) $N_{K\pi^0}$ and $N_{\pi\pi^0}$ for $B^+ \to K^+\pi^0$ and $B^+ \to \pi^+\pi^0$, and (c) $N_{K_S^0K}$ and $N_{K_S^0\pi}$ for $B^+ \to \overline{K}^0K^+$ and $B^+ \to K^0\pi^+$.

As a comparison, we relate $B \to \pi l\nu$ and $B \to \pi\pi$ processes within the factorization hypothesis. Using the ISGW II [13] form factors, the QCD factor $a_1 = 1.03 \pm 0.07$ [14], and the CLEO measurement $\mathcal{B}(B^0 \to \pi^- l^+ \nu) = (1.8 \pm 0.4 \pm 0.3 \pm 0.2) \times 10^{-4}$ [15], we predict $\mathcal{B}(B^0 \to \pi^+\pi^-) = (1.2 \pm 0.4) \times 10^{-5}$

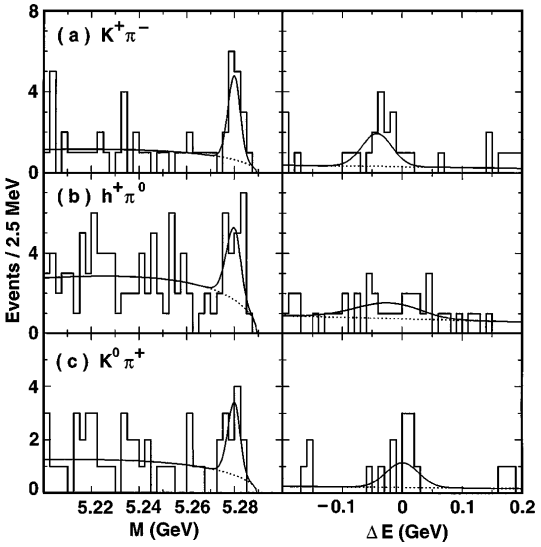

FIG. 3. M and ΔE plots for (a) $B^0 \to K^+\pi^-$, (b) $B^+ \to h^+\pi^0$, and (c) $B^+ \to K^0\pi^+$. The scaled projection of the total likelihood fit (solid curve) and the continuum background component (dotted curve) are overlaid.

and $\mathcal{B}(B^+ \to \pi^+\pi^0) = (0.6 \pm 0.2) \times 10^{-5}$ [16]. These predictions are consistent with our upper limits as well as central values from the fit: $\mathcal{B}(B^0 \to \pi^+\pi^-) = (0.7 \pm 0.4) \times 10^{-5}$ and $\mathcal{B}(B^+ \to \pi^+\pi^0) = (0.9^{+0.6}_{-0.5}) \times 10^{-5}$.

In summary, we have measured branching fractions for two of the four exclusive $B \to K\pi$ decays, while only upper limits could be established for the processes $B \to \pi\pi, KK$. Our results therefore indicate that the $b \to sg$ penguin amplitude dominates charmless hadronic B decays.

We gratefully acknowledge the effort of the CESR staff in providing us with excellent luminosity and running conditions. This work was supported by the National Science Foundation, the U.S. Department of Energy, the Heisenberg Foundation, the Alexander von Humboldt Stiftung, Research Corporation, the Natural Sciences and Engineering Research Council of Canada, and the A. P. Sloan Foundation.

*Permanent address: University of Texas, Austin, TX 78712.
†Permanent address: Lawrence Livermore National Laboratory, Livermore, CA 94551.
‡Permanent address: BINP, RU-630090 Novosibirsk, Russia.
§Permanent address: Yonsei University, Seoul 120-749, Korea.
‖Permanent address: Brookhaven National Laboratory, Upton, NY 11973.

[1] M. Kobayashi and K. Maskawa, Prog. Theor. Phys. **49**, 652 (1973).
[2] M. Gronau and D. London, Phys. Rev. Lett. **65**, 3381 (1990).
[3] R. Fleischer and T. Mannel, Phys. Rev. D **57**, 2752 (1998).
[4] M. Gronau, J. L. Rosner, and D. London, Phys. Rev. Lett. **73**, 21 (1994); R. Fleischer, Phys. Lett. B **365**, 399 (1996).
[5] CLEO Collaboration, D. M. Asner *et al.*, Phys. Rev. D **53**, 1039 (1996).
[6] ALEPH Collaboration, D. Buskulic *et al.*, Phys. Lett. B **384**, 471 (1996); DELPHI Collaboration, W. Adam *et al.*, Z. Phys. C **72**, 207 (1996).
[7] CLEO Collaboration, Y. Kubota *et al.*, Nucl. Instrum. Methods Phys. Res., Sect. A **320**, 66 (1992).
[8] S. L. Wu, Phys. Rep. C **107**, 59 (1984).
[9] R. Brun *et al.*, GEANT 3.15, CERN Report No. CERN DD/EE/84-1.
[10] G. Fox and S. Wolfram, Phys. Rev. Lett. **41**, 1581 (1978).
[11] N. G. Deshpande and J. Trampetic, Phys. Rev. D **41**, 895 (1990); L.-L. Chau *et al.*, Phys. Rev. D **43**, 2176 (1991); A. Deandrea *et al.*, Phys. Lett. B **318**, 549 (1993); **320**, 170 (1994); G. Kramer and W. F. Palmer, Phys. Rev. D **52**, 6411 (1995); D. Ebert, R. N. Faustov, and V. O. Galkin, Phys. Rev. D **56**, 312 (1997); D. Du and L. Guo, Z. Phys. C **75**, 9 (1997).
[12] ARGUS Collaboration, H. Albrecht *et al.*, Phys. Lett. B **241**, 278 (1990); Phys. Lett. B **254**, 288 (1991).
[13] N. Isgur and D. Scora, Phys. Rev. D **52**, 2783 (1995).
[14] J. Rodriguez, in Proceedings of the Conference on *B* Physics and *CP* Violation, Honolulu, 1997, edited by T. E. Browder, F. A. Harris, and S. Pakvasa (unpublished).
[15] CLEO Collaboration, J. Alexander *et al.*, Phys. Rev. Lett. **77**, 5000 (1996).
[16] The errors quoted do not include theoretical uncertainties due to the factorization hypothesis or form factors.